Vanadium incorporation from aqueous NH4VO3 solution into siliceous Beta zeolite determined by NMR with formation of V-single site zeolite catalysts for application in SCR of NO

Rafal Baran, Yannick Millot, Frederic Averseng, Stanislaw Dzwigaj

Vanadium incorporation from aqueous NH_4VO_3 solution into siliceous Beta zeolite determined by NMR with formation of V-single site zeolite catalysts for application in SCR of NO

Rafal Baran[1,2], Yannick Millot[1], Frederic Averseng[1] and Stanislaw Dzwigaj[1,*]

[1] Sorbonne Université-CNRS, Laboratoire de Réactivité de Surface, UMR 7197, 4 Place Jussieu, 75252 Paris, Cedex 05, France

[2]AGH University of Science and Technology, Faculty of Energy and Fuels, Al. A. Mickiewicza 30, 30-059 Krakow, Poland

Figures: 11

Tables: 2

Keywords: Vanadium; siliceous Beta zeolite; vanadium incorporation; NMR; SCR of NO

***Corresponding author:**

Stanislaw Dzwigaj, E-mail : stanislaw.dzwigaj@upmc.fr, tel : + 33 1 44 27 21 13

Abstract

The speciation of vanadium in initial aqueous NH_4VO_3 solutions as a function of pH and concentration, in supernatant and in wet solids were investigated by ^{51}V static and MAS NMR. Two series of VSiBeta zeolite catalysts were prepared by a two-step postsynthesis procedure at pH = 2.5 and 6. ^{51}V static and MAS NMR, ^{51}V 3Q MAS NMR, DR UV-vis, XPS and EPR allowed determining the state of vanadium in both series of catalysts. The catalytic activity of VSiBeta catalysts in SCR of NO strongly depended on the state of the vanadium present. The V-single site $V_{1.0}$SiBeta(I) and $V_{1.4}$SiBeta(I) catalysts with isolated pseudo-tetrahedral V(V) were active in SCR of NO with NH_3 process, with maximum NO conversion about 75 % at 773 K for $V_{1.4}$SiBeta(I). In contrast, $V_{1.0}$SiBeta(II) and $V_{7.5}$SiBeta(I) catalysts containing pseudo-octahedral V(V) were much less active in SCR of NO and high amount of undesired N_2O was produced.

1. Introduction

It is well known that depending on the preparation method used for incorporation of vanadium into zeolites, different vanadium species can be formed: extra-framework V species, VO_x oligomers and/or vanadium oxides and finally isolated framework V species [1]. Several studies have aimed at assigning the activity and/or selectivity of vanadium-containing zeolites to one of these species [2-7]. The question of metal speciation in the precursor solutions at different preparation conditions as well as in the zeolites after preparation of these zeolite systems have been mentioned [8-11]. It has been shown that well defined catalysts with a single type of vanadium species could be prepared by a post-synthesis method developed earlier by Dzwigaj et al. [12-14]. This method is composed of two steps. In the first step the vacant T-atom sites are created in the zeolite Beta structure by its dealumination with concentrated nitric acid and in the second step the resulting SiBeta zeolite is containing with metavanadate ammonium aqueous solution. The two-step post-synthesis method allowed incorporating vanadium in SiBeta zeolite mainly as isolated pseudo-tetrahedral V species for low vanadium content (lower than 2 V wt %) without formation of VO_x oligomers, as shown earlier by XRD, DR UV-vis and FTIR [15].

As shown earlier [16-22], the two-step post-synthesis method also allowed incorporating copper, iron and cobalt cations in the framework of the SiBeta zeolite thus obtaining Cu-, Fe- and Co-single site Beta zeolites active in selective catalytic reduction of NO into N_2. Such catalytic materials are of highly relevant importance considering that the problematic of exhaust gas cleaning is very important from many decades and has thus been the subject of many reviewers [23-29].

In this work, the speciation of vanadium in initial aqueous NH_4VO_3 solutions as a function of pH and concentration, in the supernatant after contacting siliceous Beta zeolite with aqueous NH_4VO_3 solutions and in wet solid prepared in these conditions was

investigated by ^{51}V static and MAS NMR. Two series of V-containing Beta zeolite catalysts were prepared by a two-step post-synthesis procedure. The first series with $V_{0.1}$SiBeta(I), $V_{0.5}$SiBeta(I), $V_{1.0}$SiBeta(I), $V_{1.4}$SiBeta(I) and $V_{7.5}$SiBeta(I) samples was prepared at pH = 2.5 and the second series with $V_{0.6}$SiBeta(II), $V_{1.0}$SiBeta(II) and $V_{1.6}$SiBeta(II) samples was prepared at pH = 6.

The vanadium state in both series of solids was determined by ^{51}V MAS NMR, DR UV-vis, EPR and XPS. The incorporation of V ions into the vacant T-atom sites of the framework of SiBeta zeolite as mononuclear pseudo-tetrahedral V(V) species was evidenced by combined use of XRD, FTIR, NMR and DR UV-visible. Reducibility of vanadium in V-containing Beta zeolites was investigated by EPR. The catalytic activity of V_xSiBeta(I) and V_xSiBeta(II) materials in selective catalytic reduction (SCR) of nitric oxide with ammonia as a reducing agent was investigated. It was found that SCR catalytic properties of these materials strongly depended on the state of vanadium in the Beta structure.

2. Experimental part

2.1. Material preparation

A tetraethylammonium Beta (TEABeta) zeolite with a Si/Al atomic ratio of 17, provided by RIPP (China), was dealuminated by a treatment with nitric acid solution (13 mol · L^{-1}) at 353 K for 4 h to obtain the siliceous Beta zeolite with a Si/Al atomic ratio of 1000 and was labelled SiBeta. After that, SiBeta sample was washed several times with distilled water and dried at 368 K overnight. This SiBeta sample was then contacted with aqueous NH_4VO_3 solutions of different concentrations ranging from 10^{-1} to 10^{-4} mol · L^{-1} at pH = 2.5 or pH = 6, fixed by addition of diluted HNO_3 or ammonia solutions and ^{51}V static NMR spectra of supernatant were recorded.

In addition, the siliceous Beta zeolite was also contacted with an aqueous NH_4VO_3 solution in excess, with the ratio of zeolite to solution for the first impregnation of 2g of zeolite on 200 mL of aqueous NH_4VO_3 solution with different concentrations of NH_4VO_3 varying from $0.2 \cdot 10^{-3}$ to $2.5 \cdot 10^{-2}$ mol $\cdot L^{-1}$ at pH = 2.5 or 6. The suspensions obtained at pH = 2.5 and 6 were left standing for 3 days at room temperature and then excess of water was removed with a rotary evaporator under vacuum, using a membrane pump, for 2 h at 333 K and the solids recovered. The wet solids thus obtained at pH = 2.5 contained 0.1, 0.5, 1.0, 1.4 and 7.5 V wt % and were labelled as $V_{0.1}$SiBeta(I), $V_{0.5}$SiBeta(I), $V_{1.0}$SiBeta(I), $V_{1.4}$SiBeta(I) and $V_{7.5}$SiBeta(I), accordingly. The solid obtained at pH = 6 containing 1.0 V wt % was labelled as $V_{1.0}$SiBeta(II).

Moreover, two samples with 0.6 and 1.6 V wt % were prepared in particular conditions which consists in contacting the SiBeta sample with NH_4VO_3 solutions at pH = 6 and concentrations of $1 \cdot 10^{-3}$ and $2.5 \cdot 10^{-3}$ mol $\cdot L^{-1}$ with stirring during 24 h. After that, the suspension was filtered on a Büchner funnel with a fritted glass disc and the recovered solid was washed several times with distilled water. The obtained solids were then dried in air at 353 K for 24 h and labeled $V_{0.6}$SiBeta(II) and $V_{1.6}$SiBeta(II).

$V_{0.1}$SiBeta(I), $V_{0.5}$SiBeta(I), $V_{1.0}$SiBeta(I), $V_{1.4}$SiBeta(I), $V_{0.6}$SiBeta(II) and $V_{1.6}$SiBeta(II) samples were all white, suggesting the presence of pseudo-tetrahedral V(V) species, in line with our earlier reports [30,31]. In contrast, $V_{7.5}$SiBeta(I) and $V_{1.0}$SiBeta(II) samples were pale yellow suggesting the presence of not only pseudo-tetrahedral but also pseudo-octahedral V(V) species, either as mononuclear and/or polynuclear V(V) species, in agreement with our earlier reports [30,31].

2.2. Material characterisation

An inductively coupled plasma optical emission (ICP-OES Quantima Sequential) spectrometer from GBC was used to determinate the chemical composition of the Beta zeolite

and the vanadium loading in the zeolite catalysts. Before ICP-OES analyses, the zeolites were calcined at 900 °C for 6 h and then dissolved in a mixture of HNO_3 (65%) and HF (40%) using a Milestone Ethos 1 digester. All solutions were analysed in triplicate and presented a standard deviation < 5 %. An analytical wavelength of 292.402 nm was used for the vanadium ICP-OES measurements.. Yttrium was used as an internal standard for vanadium.

^{51}V NMR spectra were recorded at 131.5 MHz on a Bruker Avance 500 spectrometer. We used a 4 mm probe for liquid and wet solid samples and a 2.5 mm probe for dry solid samples. All spectra of pure liquid phase samples are recorded in static mode while those of solid phase samples (wet or dry) are recorded by rotating the sample (Magic Angle Spinning). ^{51}V one-pulse NMR spectra of static liquid sample were acquired with 3.1 μs excitation pulse ($\pi/2$), 0.5 s for the recycle delay and from 4096 to 16384 accumulations. Wet and dry solids were spun at ν_{rot} = 12 kHz and 32 kHz, respectively. ^{51}V MAS NMR spectra were acquired with a rotor synchronized echo sequence (90°–τ–180°–τ–acq, with $\tau = 1/\nu_{rot}$) and with power levels corresponding to $\pi/2$ lengths for the liquid standard (NH_4VO_3) of 3.1 μs. A recycle time of 0.5 s was used and an accumulation between 480 and 144000 transients was performed.

^{51}V 3Q MAS spectra were acquired at ambient atmosphere with the SPAM MQMAS sequence [32]. For the two first pulses P1 and P2, the applied RF field was about 95 kHz and for the third pulse P3 it was about 6 kHz. The pulse durations P1, P2 and P3 were set empirically to 5.5, 1.5 and 10 μs respectively. We used 75 t_1 increments of 25 μs for F1 dimension acquisition and 5072 accumulations. Shearing transformation and scaling of the F1 axis was realized with "xfshear" [33]. All chemical shifts are measured by reference to solid NH_4VO_3 (δ = –570 ppm).

DR UV–vis spectra were recorded at ambient atmosphere on a Cary 5000 Varian spectrometer equipped with a double integrator by subtraction of polytetrafluoroethylene reference spectrum.

EPR spectra were recorded at ambient atmosphere on a JEOL FA-300 series EPR spectrometer operating at ≈ 9.3 GHz (X band) using a 100 kHz field modulation and a 2.5 - 5.0 Gauss standard modulation width. The spectra were recorded at 298 K (RT) and at liquid nitrogen temperature (77 K), using an insertion Dewar. Computer simulation of the spectra was performed using the EPRsim32 program [34]. A U-shaped reactor equipped of an EPR tube along with high vacuum glass-metal stoppers, allowed us to perform the thermal treatments and subsequent EPR measurements while controlling the inner pressure conditions. The as prepared samples were transferred in a suprasil tube (5 mm outside diameter) and the tube was sealed with a stopper and parafilm to avoid excess air to enter at 77 K measurements. Concerning the reduced samples, the as-prepared samples were deposited on a porous quartz disk in a U-shaped mixed quartz/glass reactor, equipped with two high vacuum glass-metal stoppers, at each end of the U tube. This U-shaped reactor presents an EPR suprasil quartz tube (5 mm ext. diameter) that permits EPR studies after treatment, by a simple powder transfer operation. The flow a H_2 (150 mL/min) was passing through the powder hold by the porous disk. After reaching 873 K (2.5 K/min), the reactor was kept at this temperature for 1 hour, then let it to cool down on its own in the tubular furnace. When room temperature was reached, the stoppers were closed, then the flow of H_2, avoiding the entrance of air/oxygen. The EPR measurements of the reduced samples were thus handled with about 1 bar of H_2 (at room temperature) in the U-shaped reactor.

X-ray photoelectron spectroscopy (XPS) measurements were performed with an Omicron (ESCA+) spectrometer, using an Al Kα ($h\nu$ = 1486.6 eV) X-ray source. The power of the X-ray source was 300 W. The area of the analyzed sample was 3 mm^2. The powder

samples were pressed on an indium foil and mounted on a special holder. Binding energy (BE) was measured by reference to the C 1s at 284.7 eV corresponding to carbon contamination. All spectra were fitted with a Voigt function (a 70/30 composition of Gaussian and Lorentzian functions) in order to determine the number of components under each XPS peak.

2.3. Catalysts activity measurements

The catalytic activity of VSiBEA zeolite catalysts in selective catalytic reduction (SCR) of NO with ammonia was carried out in a conventional fixed reactor with solid bed. Temperature was measured inside the reactor with a thermocouple and controlled with an electronic controller (LUMEL RE19). The composition of reaction mixture was: 1000 ppm NO, 1000 ppm NH_3, 3.5 vol.% O_2, 5.0 vol. % of water and He as balance. Water was added to the feed, passing helium through a saturator with deionized water. The gas mixture was fed using calibrated electronic mass flow controllers (BETA-ERG). The total gas flow was 0.1 · L min^{-1} and catalyst mass was 0.2 g. The concentration of NO and N_2O were analyzed by FTIR detectors (ABB 2000 AO series). Before the catalytic tests the samples were pretreated in oxygen/water/helium mixture (0.1 · L min^{-1}) in the temperature range 298 – 798 K with a linear heating rate of 2 K min^{-1} and then for 1 h at 798 K. The standard test conditions were 1 hour at 573 – 773 K with increasing reaction temperature every 50 K interval. The NO conversion was calculated from measured concentration of nitric oxide.

3. Results and discussion

3.1. Determination of V speciation in the aqueous NH_4VO_3 solution

It is known [35], that speciation of vanadium(V) in aqueous NH_4VO_3 solution is complex and depends on the vanadium precursor concentration and pH (Figure S1).

Vanadium(V), being a diamagnetic d° metal, is conveniently studied using ^{51}V NMR spectroscopy, electronic and vibrational spectroscopies [36-38].

We have thus applied ^{51}V static NMR to identify V speciation in the aqueous NH_4VO_3 solution in the different pH and V concentration conditions that we used during the introduction of vanadium into siliceous Beta zeolite in ambient atmosphere and also to identify the V species created in the solid in ambient atmosphere, in the further steps of preparation of V-containing siliceous Beta zeolite. From the distinctive chemical shifts of the observed lines of initial aqueous NH_4VO_3 solutions and by use of data in the literature concerning the chemistry of vanadium solutions, the vanadium species can be easily identified.

In Figures S2 and S3, two species are observed in solution (VO_2^+ and $V_{10}O_{26}(OH)_2^{4-}$) for a pH of 2.5, while five species are observed in solution ($V_4O_{12}^{4-}$, $H_2V_2O_7^{2-}$, $H_2VO_4^-$, $V_{10}O_{28}^{6-}$ and $V_5O_{15}^{5-}$) for a pH of 6. We were also able to follow precisely the variation in the relative quantity of each of these species as a function of the concentration of vanadium. To incorporate vanadium into the zeolite framework it is preferable to have small mononuclear species and ^{51}V NMR has shown that mononuclear species (VO_2^+ for pH = 2.5 and $H_2VO_4^-$ for pH = 6) are present in large relative quantities in solutions at a V concentration of 10^{-3} mol L^{-1}. Further details on the identification of vanadium species in aqueous NH_4VO_3 solutions in different pH and V concentrations can be found in Supplementary Material.

3.2. Determination of V speciation in supernatants and wet solids

After analysis of speciation of vanadium in the different pH and concentrations of initial aqueous NH_4VO_3 solutions, we have investigated the NMR spectra of supernatants and wet solids after various times of contact of aqueous NH_4VO_3 solution with siliceous Beta zeolite at different pH (2.5 and 6) and various initial concentrations of ammonium

metavanadate solutions. Figure S4 compares the ^{51}V static NMR spectra of supernatant obtained at pH = 2.5 and 6.

After 2 minutes of contact of siliceous Beta zeolite with initial aqueous NH_4VO_3 solution at pH = 2.5 and ammonium metavanadate concentration of $2.5 \cdot 10^{-3}$ mol $\cdot L^{-1}$, ^{51}V static NMR spectrum of the supernatant shows that the intensity of signal at -543 ppm characteristic of mononuclear VO_2^+ ions is much lower (Figure S4, spectrum b) than that found in initial aqueous NH_4VO_3 solution (Figure S4, spectrum a). It may indicate that VO_2^+ ions react with silanol groups present in vacant T-atom sites of siliceous Beta zeolite. Moreover, the decrease of the relative intensity of the signal at -543 ppm, characteristic of the VO_2^+ mononuclear vanadium species, compared to the intensities of the peaks at -421, -504 and -522 ppm characteristic of decavanadate $V_{10}O_{26}(OH)_2^{4-}$ complex anion shows that, in this condition, only the mononuclear V species are incorporated in the vacant T-atom sites by reaction with associated hydrogen bonded silanol groups. Increasing the contacting time of the NH_4VO_3 solution with siliceous Beta zeolite (0.5 and 1 h) lead to the complete disappearance of mononuclear VO_2^+ ions as well as polynuclear $V_{10}O_{26}(OH)_2^{4-}$ species from the solution, as shown in Figure S4, spectra c to d. Indeed, during incorporation of mononuclear VO_2^+ ions into siliceous Beta structure, the concentrations of all vanadium species in the supernatant strongly decrease, suggesting that polynuclear vanadium ions are progressively transformed in mononuclear VO_2^+ ions that are then further incorporated into siliceous Beta zeolite. Thus, we also observe the disappearance of the polynuclear vanadium species in the supernatant, owing for a long enough contacting time.

In contrast, after 1 and 2 hours contacting siliceous Beta zeolite with aqueous NH_4VO_3 solution at pH = 6 and metavanadate concentration of $2.5\ 10^{-3}$ mol $\cdot L^{-1}$ all signals related to polynuclear V, decavanadate $V_{10}O_{28}^{6-}$ (signals at about -422, -498/-500 and -514/-516 ppm),

$H_2V_2O_7^{2-}$ (signal at -570 ppm) anions and mononuclear $H_2VO_4^-$ (signal at -557 ppm) are still present in ^{51}V NMR spectrum of supernatant (Figure S4, spectra e and f).

These ^{51}V static NMR results (Figure S4) indicate that, at pH = 2.5, vanadium ions are completely incorporated into siliceous Beta zeolite after 1 h of contacting the latter with aqueous NH_4VO_3 solution (Figure S4, spectrum d) while at pH = 6, vanadium ions are still present in the supernatant even after 2 h contact with siliceous Beta zeolite (Figure S4, spectrum f).

3.3. Evidence of vanadium incorporation in the framework of SiBEA zeolite

As shown in Figure 1, already after 0.5 hour of contact of siliceous Beta zeolite with initial aqueous NH_4VO_3 solution at pH = 2.5 and ammonium metavanadate concentration of $2.5 \cdot 10^{-3}$ mol $\cdot$ L^{-1}, the ^{51}V MAS NMR spectrum of the wet solid presents a broad signal at -625 ppm (Figure 1, spectrum a) related to the formation of pseudo-tetrahedral V(V) species in the solid, in agreement with our earlier reports [7,12,13]. In contrast, at pH = 6, even after 3.5 hours of contact of siliceous Beta zeolite with initial NH_4VO_3 solution, the ^{51}V MAS NMR spectrum of wet solid only presents the signals at -417, -494 and -510 ppm related to the presence of $V_{10}O_{28}^{6-}$ complex anion (Figure 1, spectrum c). The somewhat lower values of chemical shift for this complex anion present in the wet solid (Figure 1, spectrum c) compared to that observed in the supernatant (Figure S4, spectra e-f) after 3.5 and 24 h indicate some interactions between the $V_{10}O_{28}^{6-}$ complex anion and the surface of the siliceous Beta zeolite. After 24 hours of contact of initial aqueous NH_4VO_3 solution with siliceous Beta zeolite (Figure 1, spectrum d), in addition to the signals at -417, -494 and -510 ppm, an additional signal at -553 ppm characteristic of $H_2VO_4^-$ anions appear. This chemical shift value in wet solid is a little lower than in supernatant (-557 ppm), which again suggests an interaction with the solid. Additionally, new signals at -582 and -625 ppm appear, characteristic of the polynuclear vanadium species, $V_5O_{15}^{5-}$, and mononuclear V(V) species, respectively. The

latter broad signal is related to the vanadium incorporated in the siliceous Beta zeolite as pseudo-tetrahedral V(V) species, in agreement with our earlier report on V-containing Beta zeolites [7].

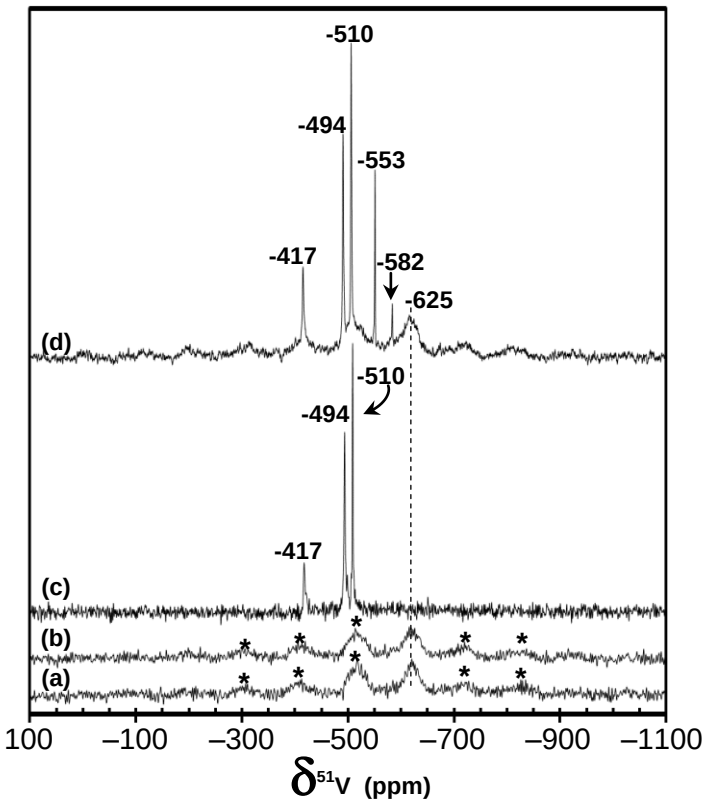

Figure 1. *^{51}V MAS NMR (12 kHz) spectra of wet solid after (a) 30 min and (b) 3.5 h of contact of siliceous Beta zeolite with $2.5 \cdot 10^{-3}$ mol $\cdot L^{-1}$ aqueous NH_4VO_3 solution at pH = 2.5 and of wet solid after (c) 3.5 h and (d) 24 h of contact of siliceous Beta zeolite with $2.5 \cdot 10^{-3}$ mol $\cdot L^{-1}$ aqueous NH_4VO_3 solution at pH = 6. The major species with their chemical shifts in ppm are $V_5O_{15}^{5-}$ (-582 ppm), $H_2VO_4^-$ (-553 ppm), $V_{10}O_{28}^{6-}$ (-510 ; -494 and -417 ppm) and framework V(V) species (-625 ppm). (*) spinning sidebands.*

Figure 2 shows the ^{51}V MAS NMR spectra of wet solid accumulated during different times of contact of $2.5 \cdot 10^{-3}$ mol $\cdot$ L^{-1} NH_4VO_3 solution at pH = 2.5 with siliceous Beta zeolite. The 15 spectra of 480 scans each, representing an accumulation time of 4 minutes per spectrum were recorded successively. As shown in Figure 2, spectrum a, after the first 4 min of contact between the siliceous Beta zeolite and the initial ammonium metavanadate solution at a concentration of $2.5 \cdot 10^{-3}$ mol $\cdot$ L^{-1} and pH = 2.5, signals at -502 and -520 ppm appeared in the spectrum. They are slightly shifted to lower values compared to that of a free $V_{10}O_{26}(OH)_2^{4-}$ ion in solution (-507 and -526 ppm) [29-30], as shown in Figure S2, spectrum a. Such shifts indicate that $V_{10}O_{26}(OH)_2^{4-}$ or $H_2V_{10}O_{28}^{4-}$ complex ions are interacting with the surface of the zeolite. The absence of the signal at -542 ppm, characteristic of mononuclear VO_2^+ cations in Figure 2, spectrum a, suggests that the latter vanadium cations present in initial aqueous NH_4VO_3 solution (Figure S2, spectrum c) are all incorporated in the siliceous Beta zeolite framework.

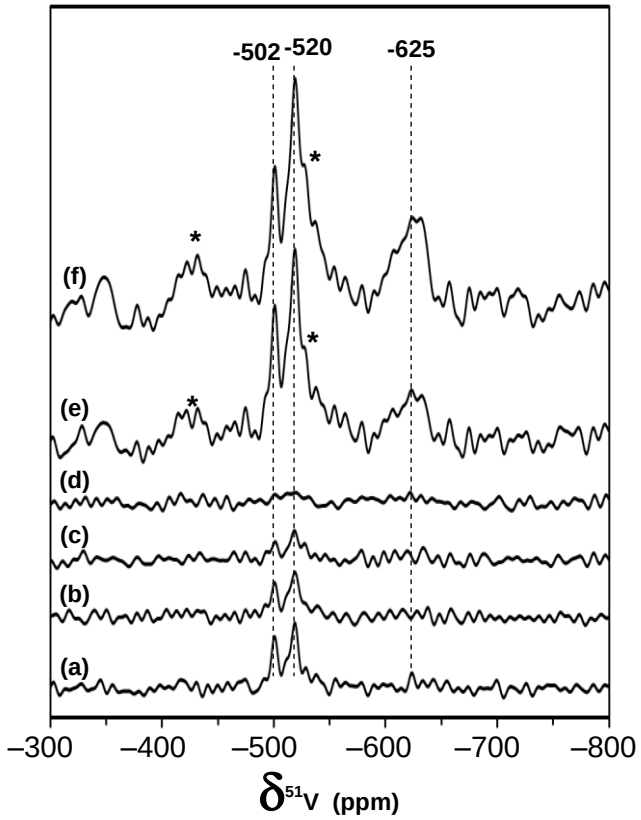

Figure 2. *^{51}V MAS NMR spectra of wet solid after contact of siliceous Beta zeolite with $2.5 \cdot 10^{-3}$ mol $\cdot$ L^{-1} aqueous NH_4VO_3 solution at pH = 2.5. 15 spectra with duration of 4 minutes (ns = 480) were continuously recorded. (a) first spectrum, (b) second spectrum, (c) third spectrum and (d) fourth spectrum. Spectrum (e) corresponds to the sum of the first 8 spectra (i.e. an accumulation time of 32 minutes, ns = 3840) and spectrum (f) corresponds to the sum of the 15 spectra (i.e. an accumulation time of 1 hour, ns = 7200). The major species with their chemical shifts in ppm are $V_{10}O_{26}(OH)_2^{4-}$ (-520 and -502 ppm) and framework V(V) species (-625 ppm). (*) spinning sidebands.*

After further accumulation of ^{51}V MAS NMR spectra of the wet solid corresponding to a contacting time of 12 to 16 min, no vanadium species are anymore observed (Figure 2, spectrum d) suggesting that all vanadium is incorporated in the solid and is therefore not present in the liquid phase of wet solid. The spectrum e of Figure 2 corresponds to the addition of the first 8 spectra, i.e. an overall spectrum of 3840 scans with a total accumulation time of 32 minutes. The spectrum present three signals at -502, -520 and -625 ppm (Figure 2, spectrum e) related to polynuclear $V_{10}O_{26}(OH)_2^{4-}$ anion (signals at -502 and -520 ppm), present in the initial contacting solution and mononuclear (signal at -625 ppm) framework vanadium(V) species, in line with our earlier report [7]. Further accumulation of ^{51}V spin (sum of 15 spectra i.e. 7200 scans and an accumulation time of 64 minutes) lead to increasing the intensity of the signals at -502, -520 and -625 ppm (Figure 2, spectrum f) confirming the presence in the wet solid of polynuclear and mononuclear V(V) species.

The ^{51}V MAS NMR spectra of dry $V_{0.1}$SiBeta(I) and $V_{0.5}$SiBeta(I) solids after 72 h of preparation in NH_4VO_3 solution at pH = 2.5 (Figure 3, spectra a and b) present one signal at –625 ppm ($V^V_{(a)}$) characteristic of pseudo-tetrahedral V(V) species, in line with our earlier

reports [7,12,13]. For $V_{1.0}$SiBeta(I) and $V_{1.4}$SiBeta(I), a second peak ($V^{V}_{(b)}$) appears at -585 ppm (Figure 3, spectra c and d) related to a second kind of pseudo-tetrahedral V(V). Upon increasing the concentration of vanadium in the initial aqueous NH_4VO_3 solution up to $2.5 \cdot 10^{-2}$ mol $\cdot L^{-1}$ at pH=2.5, pseudo-octahedral V(V) species are formed in $V_{7.5}$SiBeta(I) sample evidenced by the signal at -542 ppm, in addition to pseudo-tetrahedral V(V) species with signals at -625 and -585 ppm, as shown in Figure 3, spectrum e.

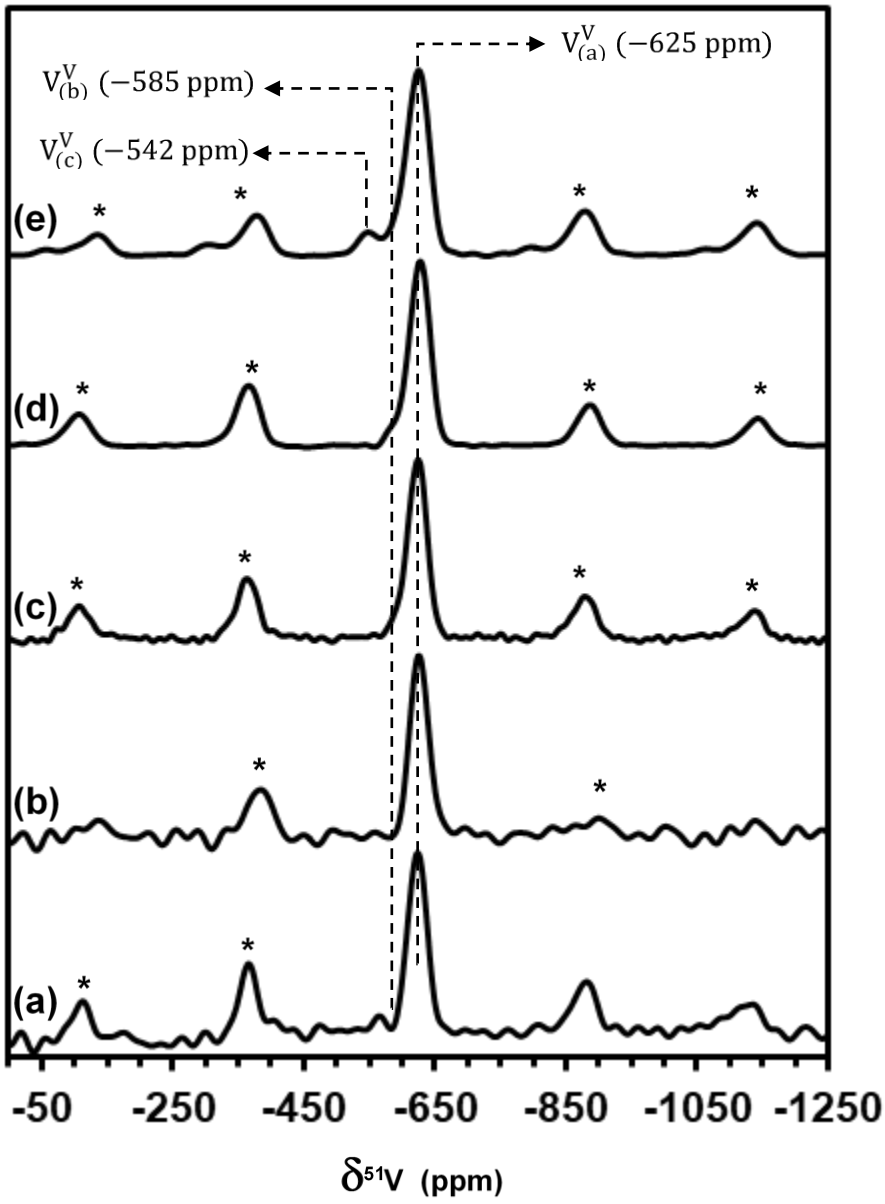

Figure 3. *^{51}V MAS NMR spectra recorded at ambient condition of dry solid (a) $V_{0.1}$SiBeta(I),*

(b) $V_{0.5}$SiBeta(I), (c) $V_{1.0}$SiBeta(I), (d) $V_{1.4}$SiBeta(I) and (e) $V_{7.5}$SiBeta(I) after 72 hours of contact of siliceous Beta zeolite with aqueous NH_4VO_3 solution at pH = 2.5. The spectra were recorded in 2.5 mm diameter zirconia sample holder with spinning of 32 kHz. (*) spinning sidebands.

The ^{51}V 3Q MAS NMR spectrum of $V_{1.0}$SiBeta(I) (Figure 4) shows that these two peaks follow the diagonal of the 2D spectrum (chemical shift axis) and correspond to two different framework V in pseudo-tetrahedral environments with weak quadrupole coupling. Our earlier investigation [39] has revealed the presence in parent Beta zeolite of two kinds of tetrahedral Al(III) species with particular environments in the framework of the zeolite structure. So, when vanadium is incorporated in the vacant T-atom sites of Beta zeolite formed by removal of these two kinds of tetrahedral Al(III), also two kinds of pseudo-tetrahedral V(V) species are formed upon contact with NH_4VO_3 solution at pH = 2.5, $V^V_{(a)}$) and $V^V_{(b)}$), as shown in Figure 4.

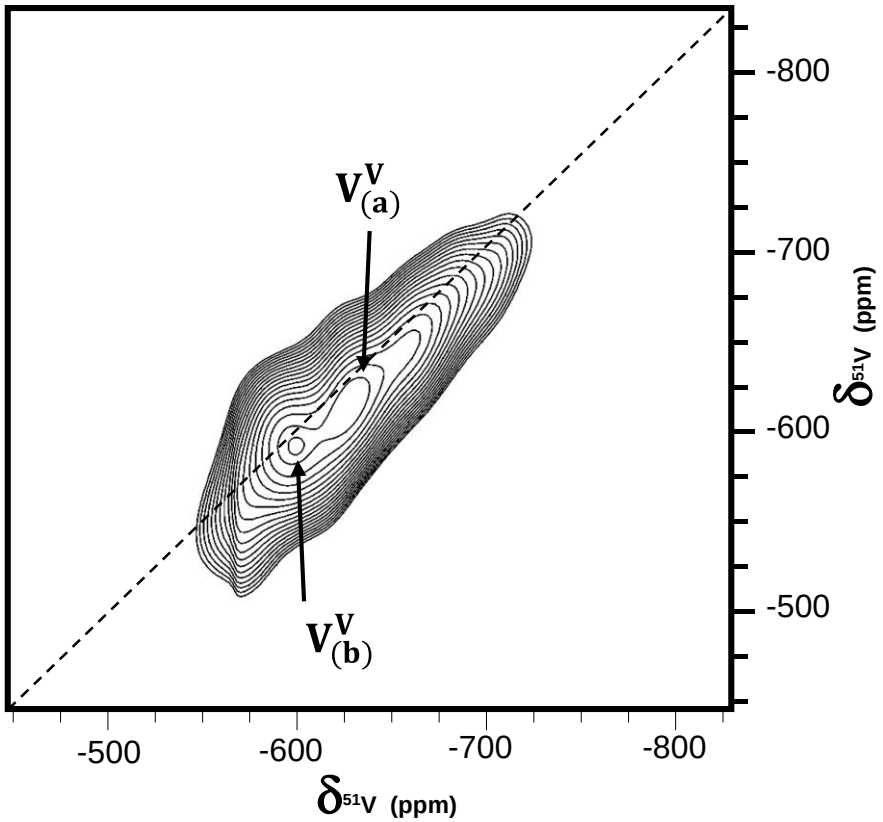

Figure 4. *^{51}V 3Q MAS NMR spectra recorded at ambient condition of dry solid $V_{1.0}$SiBeta(I) after 72 hours of contact of siliceous Beta zeolite with $2.5 \cdot 10^{-3}$ mol $\cdot$ L^{-1} aqueous NH_4VO_3 solution at pH = 2.5.*

In the ^{51}V MAS NMR spectra of dry $V_{0.6}$SiBeta(II), $V_{1.0}$SiBeta(II) and $V_{1.6}$SiBeta(II) solids after 72 h of preparation in NH_4VO_3 solution at pH = 6 (Figure 5, spectra a, b and c, respectively) only one signal is observed ($V^{V}_{(a)}$) at – 625 ppm characteristic of pseudo-tetrahedral V(V) species. It suggests that during the preparation of these solids at pH = 6 only one kind of pseudo-tetrahedral V(V) is formed in the zeolite Beta structure, related to particular condition of preparation: while VO_2^+ was the main species in the initial aqueous NH_4VO_3 solution at pH = 2.5, it is now $H_2VO_4^-$ at pH = 6, in agreement with Figure S1.

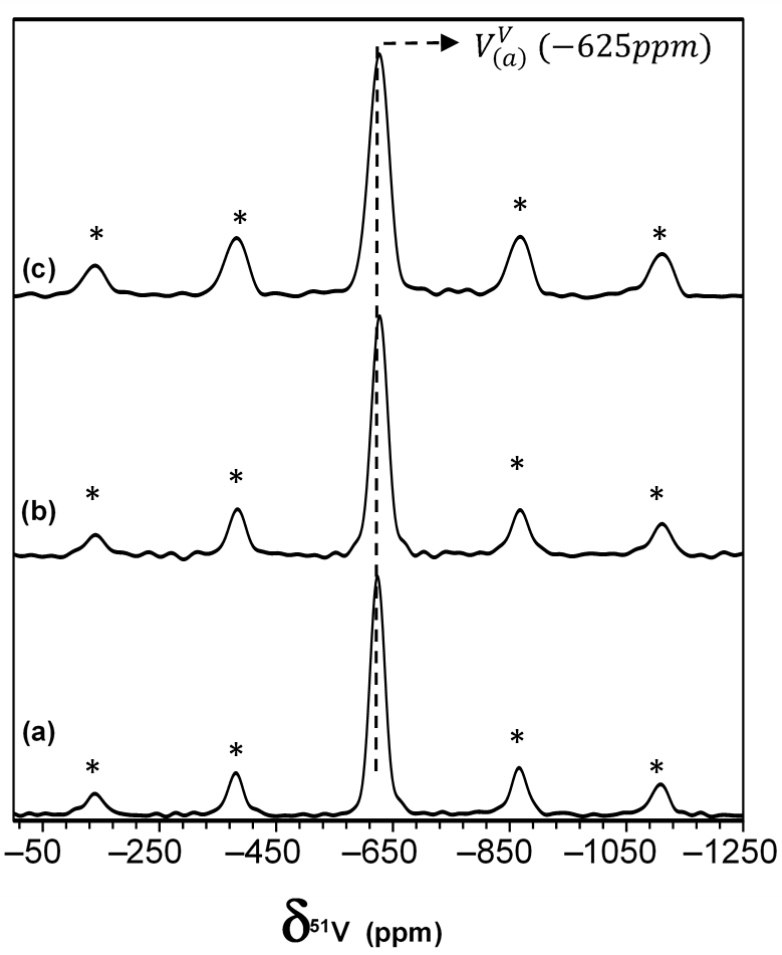

Figure 5. *^{51}V MAS NMR spectra recorded at ambient atmosphere of dry solid (a) $V_{0.6}$SiBeta(II), (b) $V_{1.0}$SiBeta(II) and (c) $V_{1.6}$SiBeta(II) after 72 hours of contact of siliceous Beta zeolite with aqueous NH_4VO_3 solution at pH = 6. The spectra recorded in 2.5 mm diameter zirconia sample holder with spinning of 32 kHz. (*) spinning sidebands.*

In both cases (pH = 2.5 and 6), vanadium can be incorporated into the zeolite as mononuclear pseudo-tetrahedral V species but more quickly at pH = 2.5 than at pH = 6. This difference can be explained by the electronic charge of the major species contained in the initial solution, cation VO_2^+ at pH = 2.5 and anion $H_2VO_4^-$ at pH = 6. Indeed, the vacant T-atom sites, negatively charged at pH higher than 2, will thus favor the incorporation of cationic V species at pH of 2.5.

The state of the vanadium present in V_xSiBeta(I) and V_xSiBeta(II) after different treatments, i.e. calcination in oxygen at 773 K and treatment at 873 K in hydrogen, were also investigated by DR UV-vis, and EPR spectroscopies.

The DR UV-vis measurements were carried out for as prepared (Figure 6a) and calcined (Figure 6b) $V_{0.1}$SiBeta(I), $V_{0.5}$SiBeta(I), $V_{1.0}$SiBeta(I) and $V_{1.4}$SiBeta(I) as well as for as prepared (Figure 7a) and calcined (Figure 7b) $V_{0.6}$SiBeta(II), $V_{1.0}$SiBeta(II) and $V_{1.6}$SiBeta(II) samples.

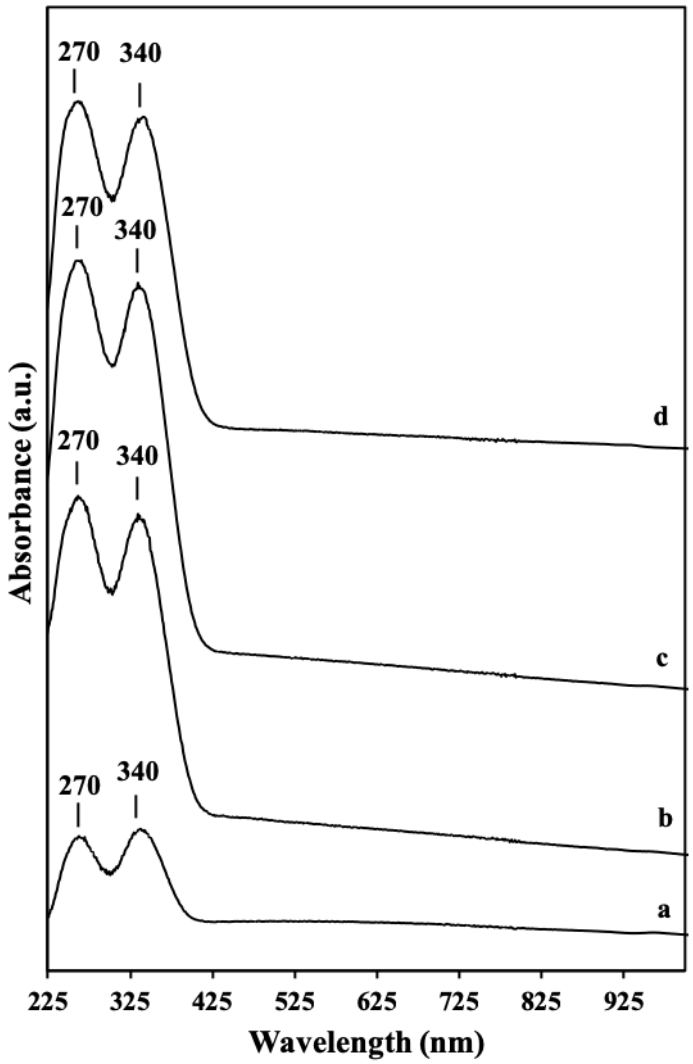

***Figure 6a**. DR UV-vis spectra recorded at ambient atmosphere of dry solid (a) $V_{0.1}$SiBeta(I), (b) $V_{0.5}$SiBeta(I), (c) $V_{1.0}$SiBeta(I) and (d) $V_{1.4}$SiBeta(I) after 72 hours of contact of siliceous*

Beta zeolite with aqueous NH_4VO_3 solution at pH = 2.5.

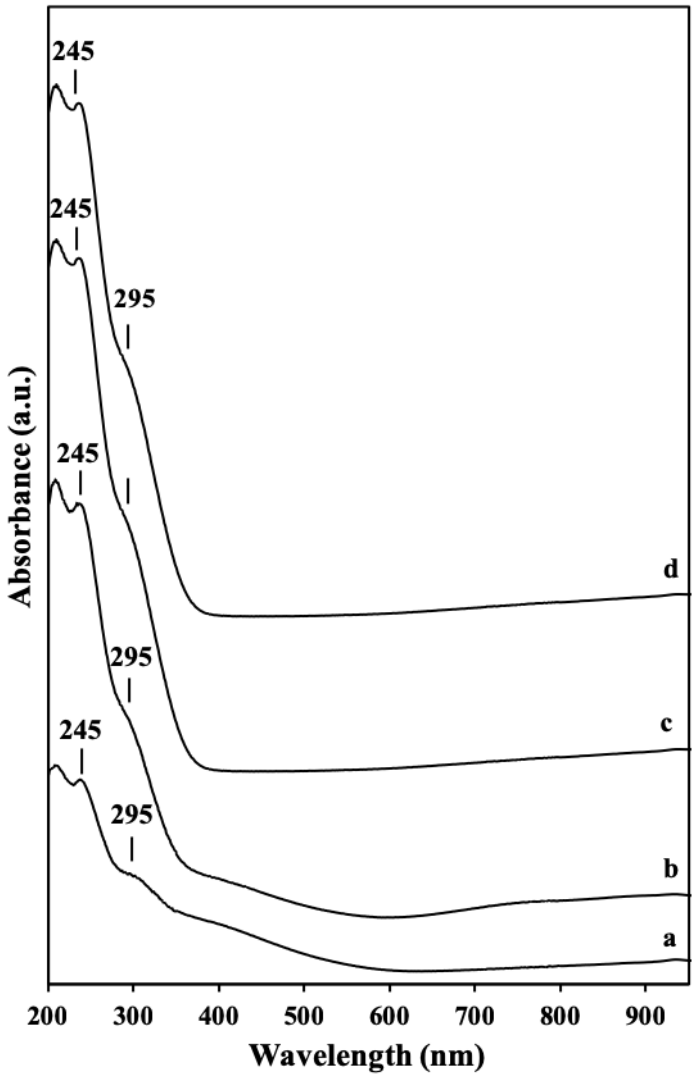

***Figure 6b**. DR UV-vis spectra recorded at ambient atmosphere of calcined in air at 773 K for 3h (a) $V_{0.1}$SiBeta(I), (b) $V_{0.5}$SiBeta(I), (c) $V_{1.0}$SiBeta(I) and (d) $V_{1.4}$SiBeta(I) after 72 hours of contact of siliceous Beta zeolite with aqueous NH_4VO_3 solution at pH = 2.5.*

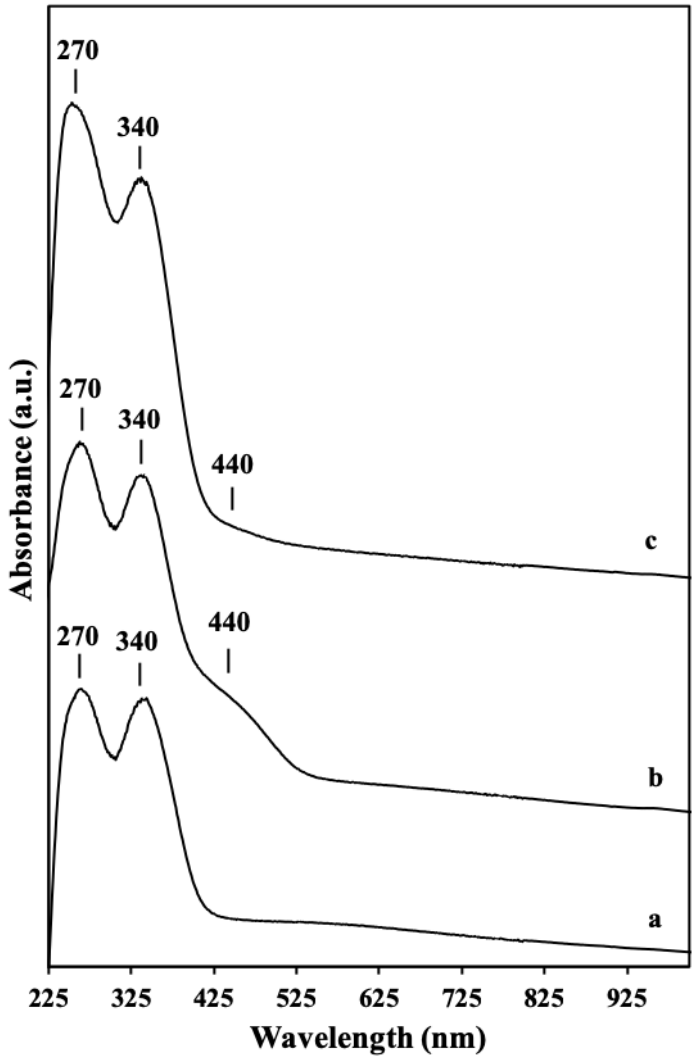

Figure 7a. *DR UV-vis spectra recorded at ambient atmosphere of dry solid (a) $V_{0.6}$SiBeta(II), (b) $V_{1.0}$SiBeta(II) and (c) $V_{1.6}$SiBeta(II) after 72 hours of contact of siliceous Beta zeolite with aqueous NH_4VO_3 solution at pH = 6.*

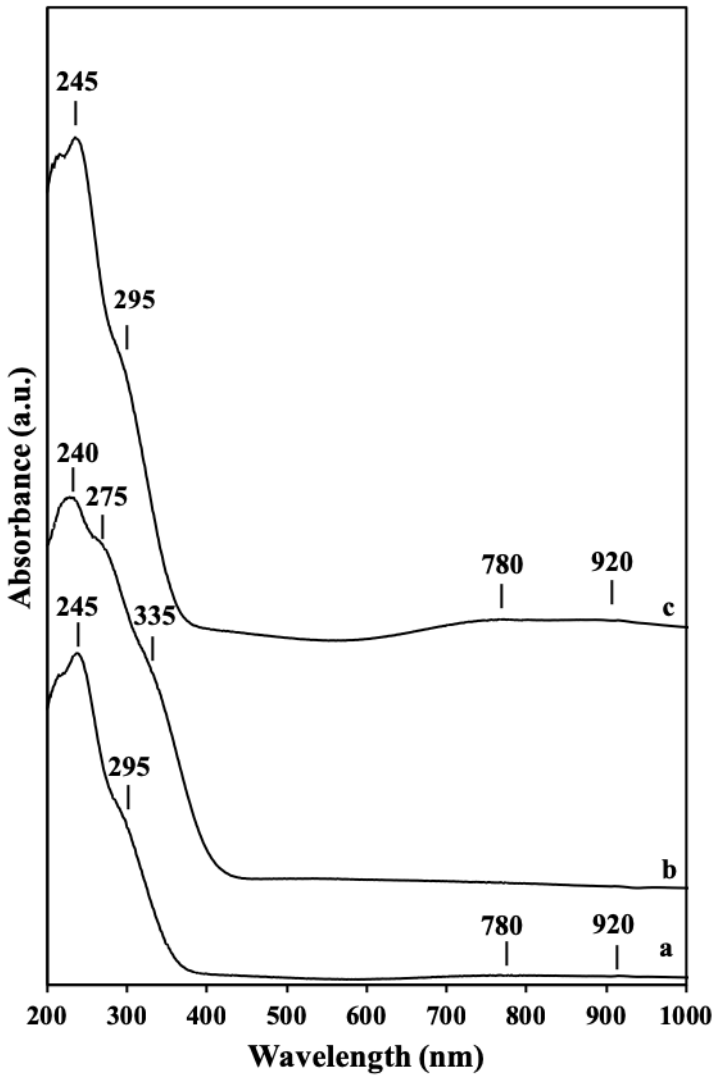

Figure 7b. *DR UV-vis spectra recorded at ambient atmosphere of calcined in air at 773 K for 3 h (a) $V_{0.6}$SiBeta(II), (b) $V_{1.0}$SiBeta(II) and (c) $V_{1.6}$SiBeta(II) after 72 hours of contact of siliceous Beta zeolite with aqueous NH_4VO_3 solution at pH = 6.*

The DR UV-vis spectra of as prepared $V_{0.1}$SiBeta(I), $V_{0.5}$SiBeta(I), $V_{1.0}$SiBeta(I) and $V_{1.4}$SiBeta(I) (Figure 6a, spectra a to d) and $V_{0.6}$SiBeta(II) (Figure 7a, spectrum a) exhibit two main bands at 270 and 340 nm attributed to oxygen-to-pseudo-tetrahedral V(V) charge transfer transitions, involving oxygen in bridging (V-O-Si) and terminal (V=O) positions, respectively, in line with earlier reports [39-40]. In contrast, while for as prepared

$V_{1.0}$SiBeta(II) and $V_{1.6}$SiBeta(II) the main bands at 270 and 340 nm are also present, an additional band at 400 nm appears, related to oxygen-to-pseudo-octahedral V(V) charge transfer transitions (Fig. 7a, spectra b and c), in line with our earlier works [39-41]. It clearly shows that the kind of procedure used for the preparation of V_xSiBeta(I) and V_xSiBeta(II) series of samples has a significant influence on the nature and environment of vanadium species incorporated in SiBeta support.

The DR UV-vis spectra of calcined $V_{0.1}$SiBeta(I), $V_{0.5}$SiBeta(I), $V_{1.0}$SiBeta(I), $V_{1.4}$SiBeta(I) (Fig. 6b, spectra a to d) and calcined $V_{0.6}$SiBeta(II) (Fig. 7b, spectrum a) exhibit two bands at 245 and 295 nm. The shift of these DR UV-vis charge-transfer bands to lower wavelengths upon calcination suggests a greater distortion of pseudo-tetrahedral V(V) species in calcined samples than that in as prepared ones, in agreement with earlier work [30-31]. In contrast, two main bands appear at 245 and 275 nm for calcined $V_{1.0}$SiBeta(II) and at 245 and 295 nm for $V_{1.6}$SiBeta(II) (Fig. 7b, spectra b and c, respectively) attributed to oxygen-to-pseudo-tetrahedral V(V) charge transfer transitions, involving oxygen in bridging (V-O-Si) and terminal (V=O) positions, respectively with a shoulder at about 335 nm attributed to oxygen-to-pseudo-octahedral V(V) charge transfer transition. The shift of the DR UV-vis charge-transfer bands attributed to pseudo-tetrahedral V(V) and pseudo-octahedral V(V) species after calcination of $V_{1.0}$SiBeta(II) and $V_{1.6}$SiBeta(II) suggests a greater distortion than that in as prepared samples.

XPS spectrum of as prepared $V_{1.0}$SiBeta(I) sample (Fig. S5, spectrum a) dried at 473 K contains one symmetric peak in both V $2p_{3/2}$ and V $2p_{1/2}$ ranges, suggesting the presence of one type of vanadium surface species. These two ranges of BE values of V $2p_{3/2}$ and V $2p_{1/2}$ show that vanadium in this sample is present in (V) oxidation state. The appearance of the peaks for V $2p_{3/2}$ and V $2p_{1/2}$ at BE values of 516.8 and 524.1 eV, respectively, seems to indicate the main presence in this sample of pseudo-tetrahedral V(V) species, in line with

earlier reports [43-46]. The decrease of the intensity of these two peaks for $V_{1.0}$SiBeta(I) sample, calcined at 773 K in air (Figure S5, spectrum b), without changing the BE values suggests that the tetrahedral environment of vanadium in the framework position is not significantly changed upon calcination. After treatment of calcined $V_{1.0}$SiBeta(I) sample in hydrogen at 873 K (Figure S5, spectrum c), one can only observe a little diminution of the intensity of the band at 517.1 eV which suggests that only part of pseudo-tetrahedral V(V) is reduced to V(IV) for this sample.

In contrast, the appearance of asymmetric peaks in both V $2p_{3/2}$ and V $2p_{1/2}$ ranges for as prepared $V_{1.0}$SiBeta(II) dried at 473 K suggests the presence of two types of vanadium surface species (Figure S6). The less intense contributions for V $2p_{3/2}$ and V $2p_{1/2}$ peak at BE values of 516.1 and 523.4 eV, respectively, are consistent with the presence of pseudo-tetrahedral V(V) species in this sample. However, the second, more intense contributions peaking for V $2p_{3/2}$ and V $2p_{1/2}$ at BE values of 517.2 and 524.5 eV, respectively, reveal that another type of V(V) species is also present in $V_{1.0}$SiBeta(II) sample. These values may be ascribed to pseudo-octahedral V(V), in agreement with DR UV-vis results (Fig. 7a). The decrease of the intensity of the latter two peaks for calcined $V_{1.0}$SiBeta(II) sample attributed to pseudo-octahedral V(V) with a shift to higher BE values (from 517.2 to 518.3 eV and from 524.5 to 525.5 eV, respectively) with the simultaneous increase of intensity of the peaks close at 516.5 and 523.7 eV, attributed to pseudo-tetrahedral V(V), indicates that part of the polynuclear V(V) species is transformed into mononuclear V(V) one upon calcination in air at 773 K and is incorporated in the structure of Beta zeolite as pseudo-tetrahedral V(V). After treatment of calcined $V_{1.0}$SiBeta(II) sample in hydrogen at 873 K, one can observe the disappearance of the peak at 518.3 eV and 525.5 attributed to polynuclear V(V), which suggests that this species is easy reduced and the diminution of the intensity of the bands close to 517 and 524 eV (Figure S6) suggests that pseudo-tetrahedral V(V) in this sample are

more easily reduced than the pseudo-tetrahedral V(V) present in $V_{1.0}$SiBeta(I). It suggests that the pseudo-tetrahedral V(V) species in the $V_{1.0}$SiBeta(II) less strongly interact with the zeolite structure than the pseudo-tetrahedral V(V) ones present in $V_{1.0}$SiBeta(I). It is important to mention here that V/Si ratio obtained from XPS measurement for $V_{1.0}$SiBeta(II) is significantly higher than that for $V_{1.0}$SiBeta(I) for as prepared, calcined as well as for reduced samples (Table 1). These XPS results combined with DR UV-vis strongly indicate that incorporation of vanadium in SiBeta is less favoured at pH = 6 that at pH = 2.5 and thus accumulate on the surface of the zeolite. This is related to the presence of $H_2VO_4^-$ mononuclear ions in the aqueous solution of NH_4VO_3 at pH = 6 (see Figure S1 and Figure S4, spectra e and f). Thus, in this condition, a strong interaction of negatively charged $H_2VO_4^-$ ions with the negatively charged vacant T-atom sites with associated silanols in the first step of preparation is highly improbable. Therefore, at pH = 6, incorporation of vanadium is very slow as it is shown by ^{51}V static NMR spectra in Figure S4 and vanadium is mainly located in the extra-framework position. In contrast, conditions for the incorporation of vanadium at pH = 2.5 are much more advantageous, as shown by Figure S1 and Figure S4, spectra a-d). Indeed, positively charged VO^+ ion very favourably and quickly interacts with the negatively charged surface, in particular with the silanol groups of vacant T-atom sites even at room temperature and rapidly form pseudo-tetrahedral V(V) species (see Figure S4, spectra a-d and Figure 6a).

Table 1. XPS characteristics of $V_{1.0}$SiBeta(I) and $V_{1.0}$SiBeta(II) after various treatments.

Sample	V $2p_{3/2}$ peak positions		V/Si ratio
$V_{1.0}$SiBeta(I)*	516.8		0.008
Calcined $V_{1.0}$SiBeta(I)	517.1		0.004
Reduced $V_{1.0}$SiBeta(I)	517.1		0.002
$V_{1.0}$SiBeta(II)*	517.2	516.1	0.014
Calcined $V_{1.0}$SiBeta(II)	518.3	516.5	0.023
Reduced $V_{1.0}$SiBeta(II)	516.9		0.014

* to remove excess of water, samples were dried ex-situ at 473 K before the analysis

3.4. Reducibility of vanadium species present in VSiBeta zeolites

The EPR spectra of $V_{1.0}$SiBeta(I) prepared at pH = 2.5 do not exhibit any signal whatever the measurement temperature (298 K: Figure 8, spectrum a and 77 K: Figure 8, spectrum c), thus excluding the presence of any V(IV) species. After reducing under treatment with H_2 flowing at 873 K, the EPR spectrum recorded at 298 K (Figure 8, spectrum b) reveals a weak signal with hyperfine splitting, that can be assigned to very small amounts of V(IV) species formed, most probably in a distorted octahedral environment, in line with earlier reports [10,47-48]. Upon cooling the sample down to 77 K (Figure 8, spectrum d), the EPR spectrum reveals an intense signal, typical of V(IV). This signal presents an axial symmetry. While $g_{\parallel}$ and $A_{\parallel}$ values can be precisely obtained by simulation, $g_{\perp}$ and $A_{\perp}$ can only be estimated, due to the broadness of the peaks. Yet the values reported in Table 2, and the fact that this specific V(IV) signal is only observed at 77 K, strongly points out to the presence of pseudo-tetrahedral V(IV) species, in line with earlier report [49]. Indeed, such d^1 species are known to present small relaxation times, due to the presence of low-lying states, thus making them observable by EPR at low temperatures only (100 K or lower).

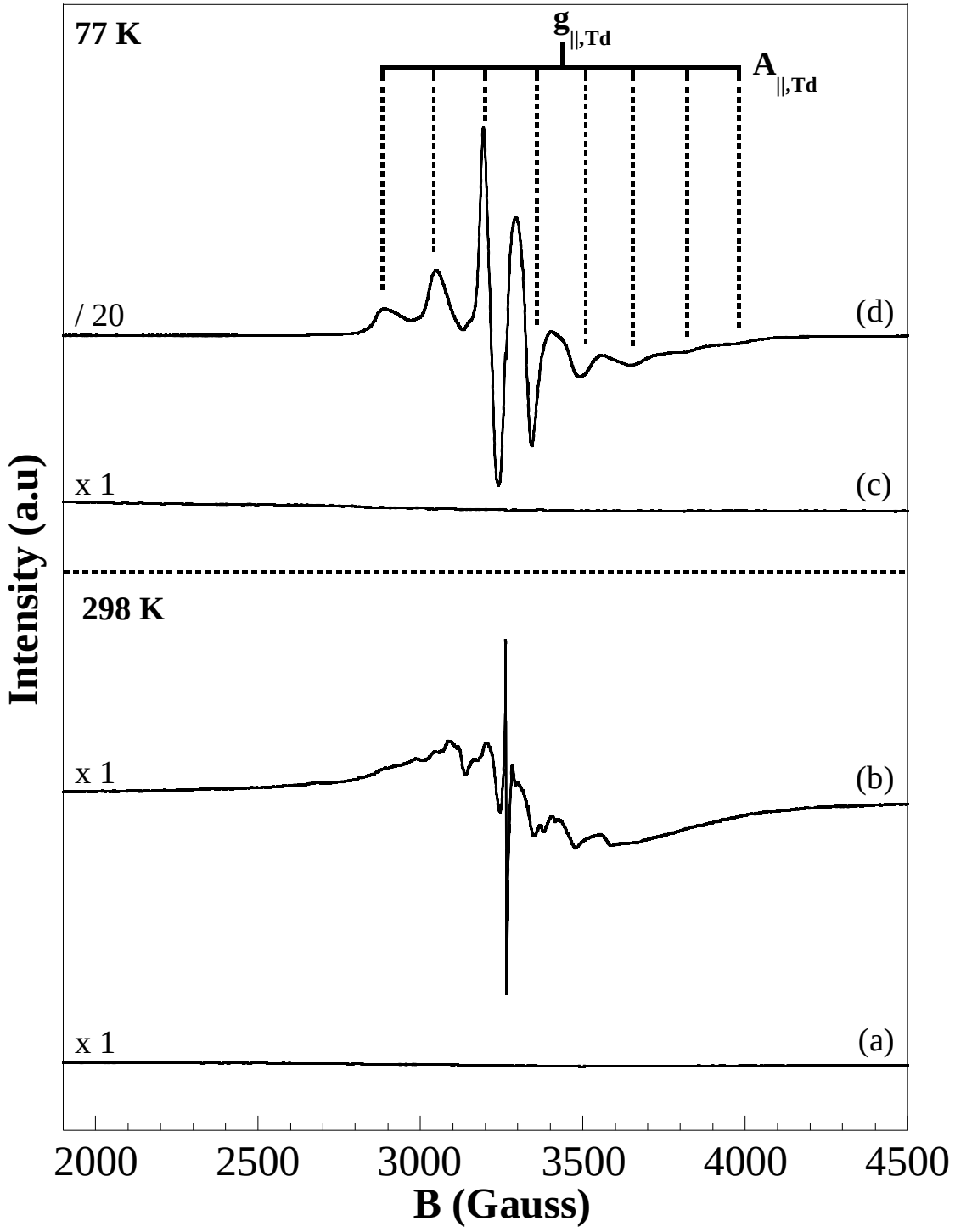

Figure 8. *EPR spectra of as prepared $V_{1.0}$SiBeta(I) recorded at ambiant atmosphere (a) and 77 K (c) and reduced $V_{1.0}$SiBeta(I) in H_2 at 873 K for 1 h recorded at room temperature (b) and 77 K (d), respectively.*

The EPR spectra of $V_{0.6}$SiBeta(II) prepared at pH = 6.0 (presents very weak signals at 298 K (Figure 9, spectrum a) and 77 K (Figure 9, spectrum c), indicating very small amounts of V(IV) in the prepared zeolite. After reducing under treatment with H_2 flowing at 873 K, the EPR spectrum recorded at 298 K present a weak signal of pseudo-octahedral V(IV) species (Figure 9, spectrum b), similar to that of $V_{1.0}$SiBeta(I) prepared at pH = 2.5 (Figure 8, spectrum b). Once again, cooling down the sample to 77 K reveals a very intense signal of pseudo-tetrahedral V(IV) species (Figure 9, spectrum d). This signal with similar g and A values to that of $V_{1.0}$SiBeta(I) prepared at pH = 2.5 (Table 2), points out a similar environment of V(IV) in both zeolites. One can thus state that in both zeolite samples the majority of V(IV) species, formed upon reduction under treatment with H_2 flowing at 873 K, are pseudo-tetrahedral ones. A close comparison of EPR spectra after reduction (Figure 8, spectrum d and Figure 9, spectrum d) indicates a slightly broader signal for $V_{1.0}$SiBeta(I) prepared at pH = 2.5, pointing out a somewhat higher heterogeneity of V(IV) species (bringing out higher g- and A-strain), which may be due to slightly different V environment in the samples prepared at pH = 2.5 and 6.0. This is consistent with NMR results which revealed two kinds of pseudo-tetrahedral V(V) species in the case of $V_{1.0}$SiBeta(I) prepared at pH = 2.5 and only one for $V_{0.6}$SiBeta(II) prepared at pH = 6.0 (Figures 3 and 6).

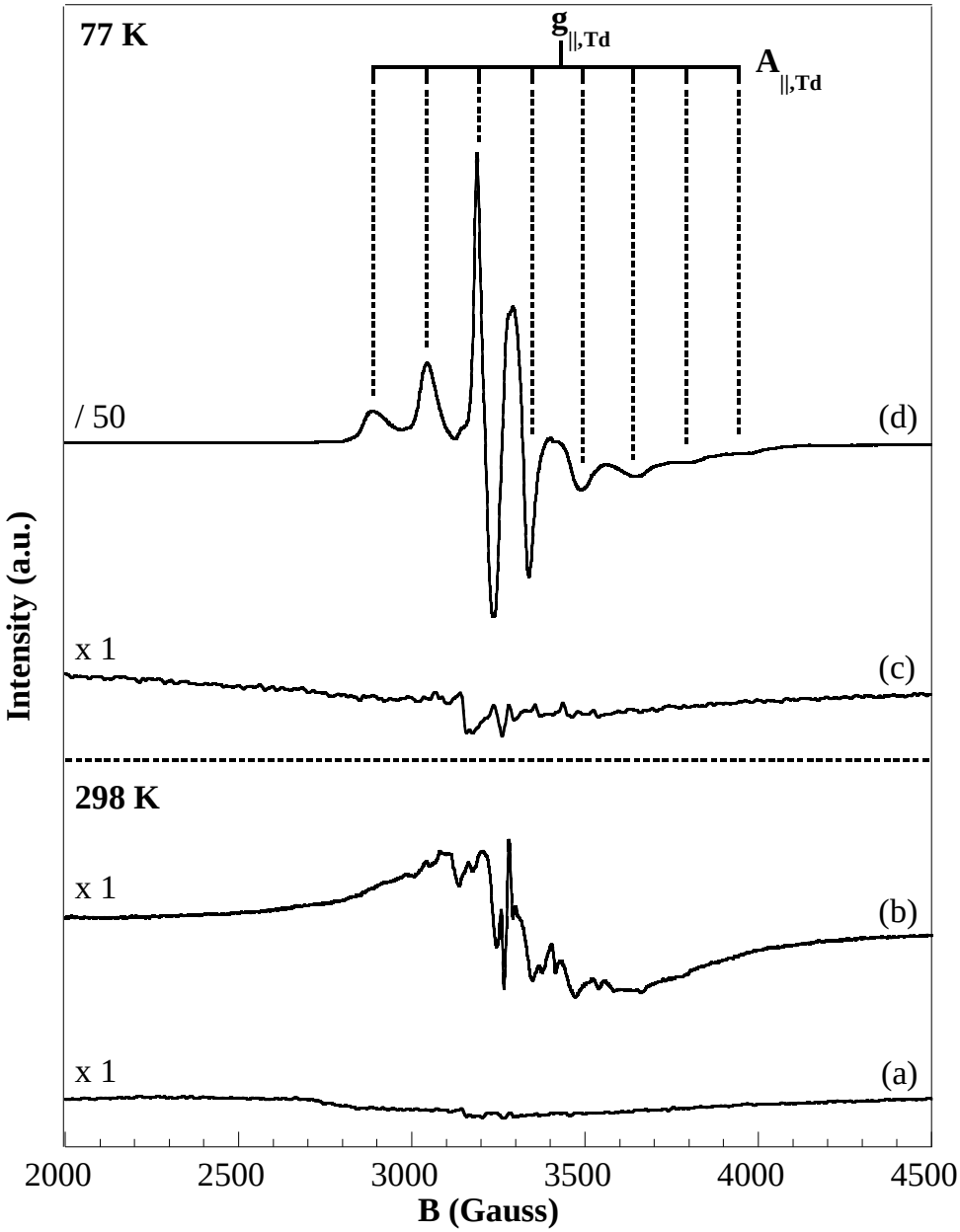

Figure 9. *EPR spectra of as prepared $V_{0.6}$SiBeta(II) recorded at ambiant atmosphere (a) and 77 K (c) and reduced $V_{0.6}$SiBeta(II) in H_2 at 873 K for 1 h recorded at room temperature (b) and 77 K (d), respectively.*

The EPR spectra of $V_{1.0}$SiBeta(II) prepared at pH = 6.0 do not exhibit any signal, whatever the measurement temperature (298 K: Figure S7, spectrum a and 77 K: Figure S7, spectrum b), thus excluding the presence of any V(IV) species in the as-prepared material. After reducing under treatment with H_2 flowing at 873 K, the EPR spectrum recorded at 298

K present a complex signal composed of many hyperfine lines typical of V(IV) species (Figure S7, spectrum c). The main signal can be unambiguously assigned to distorted pseudo-octahedral V(IV) species (positions of $g_{||}$ and $A_{||}$ hypefine lines are presented in blue, Figure S7), referred to as species A. Yet additional V(IV) species must be considered to fully simulate the spectrum. Values and contributions of each species are presented in Table 2. The $g_{||}$ and $A_{||}$ lines positions of each species are presented in Figure S7: the red one, species B, corresponds to another distorted octahedral V(IV) species while the orange, species C, presents some unusual $g_{||}$ (similar to that of a Td species) and $A_{||}$ (similar to that of a distorted Oh species) values requiring 77 K measurement for additional information. Indeed, the spectrum obtained at 77 K (Figure S7, spectrum d), though similar to that of 298 K, presents some useful differences: (i) the relative intensities of A (blue) and B (red) species (both in a distorted octahedral environment) present a similar ratio. This is not true for the C (orange) V(IV) species which peaks are relatively more intense compared to that of A and B species (especially visible at low magnetic field). This indicates a smaller relaxation time for the species C, yet not as small as that for a Td species, which would remain silent at 298 K. We can thus propose some intermediate geometry between a distorted Oh and a distorted Td for V(IV) species C (orange). Additional peaks (green) should also be considered at 77 K. The fact that such peaks weren't observed at 298 K and that the $g_{||}$ and $A_{||}$ values of this species, presented in the Table 2, are very similar to that observed for $V_{0.6}$SiBeta(II) and $V_{1.0}$SiBeta(II) allows us to state that the green signal (species D) arises from pseudo-tetrahedral V(IV) species. One should note that, contrary to $V_{1.0}$SiBeta(I) prepared at pH = 2.5 and $V_{0.6}$SiBeta(II) prepared at pH = 6, only a small fraction of V(IV) formed after reduction under treatment with H_2 flowing at 873 K is pseudo-tetrahedral, the majority exhibiting a pseudo-octahedral environment. This is not surprising as DR-UV pointed out the noticeable presence of pseudo-octahedral V(V) only in the case of V_xSiBeta(II) prepared at pH = 6, with $x \geq 1.0$.

Table 2. Simulated EPR parameters of isolated V^{IV} species in $V_{1.0}$SiBeta(I) prepared at pH = 2.5 and in $V_{0.6}$SiBeta(II) and $V_{1.00}$SiBeta(II) prepared at pH = 6.

Sample	EPR parameters					Species	Environment
	$g_{\parallel}$	$A_{\parallel}$	$g_{\perp}$	$A_{\perp}$	Signal		
$V_{1.0}$SiBeta(I) (pH = 2.5)	1.900 ± 0.004	148 ± 4 G	1.956 ± 0.003	40 G ± 12 G	77 K	Main	Td
$V_{0.6}$SiBeta(II) (pH = 6)	1.900 ± 0.002	150 ± 4 G	1.963 ± 0.003	33 ± 10 G	77 K	Main	Td
$V_{1.0}$SiBeta(II) (pH = 6)	1.936 ± 0.001	192 ± 1 G	1.968 ± 0.003	64 ± 4 G	298 and 77 K	Main (A)	Oh
	1.927 ± 0.002	203 ± 1 G	1.97 ± 0.01	65 ± 4 G	298 and 77 K	Minor (B)	Oh
	1.87 ± 0.01	190 ± 10 G	1.91 ± 0.01	35 ± 10 G	298 and 77 K	Minor (C)	Intermediate Oh-Td
	1.900 ± 0.004	150 ± 5 G G	1.97 ± 0.01	37 ± 10 G	77 K	Minor (D)	Td

3.5. Catalytic activity of VSiBEA zeolite catalysts

Two series of V-containing SiBeta zeolite catalysts were investigated in SCR of NO with ammonia and their catalytic performances, NO conversion and N_2O formation, are illustrated by Figures 10 and 11, respectively.

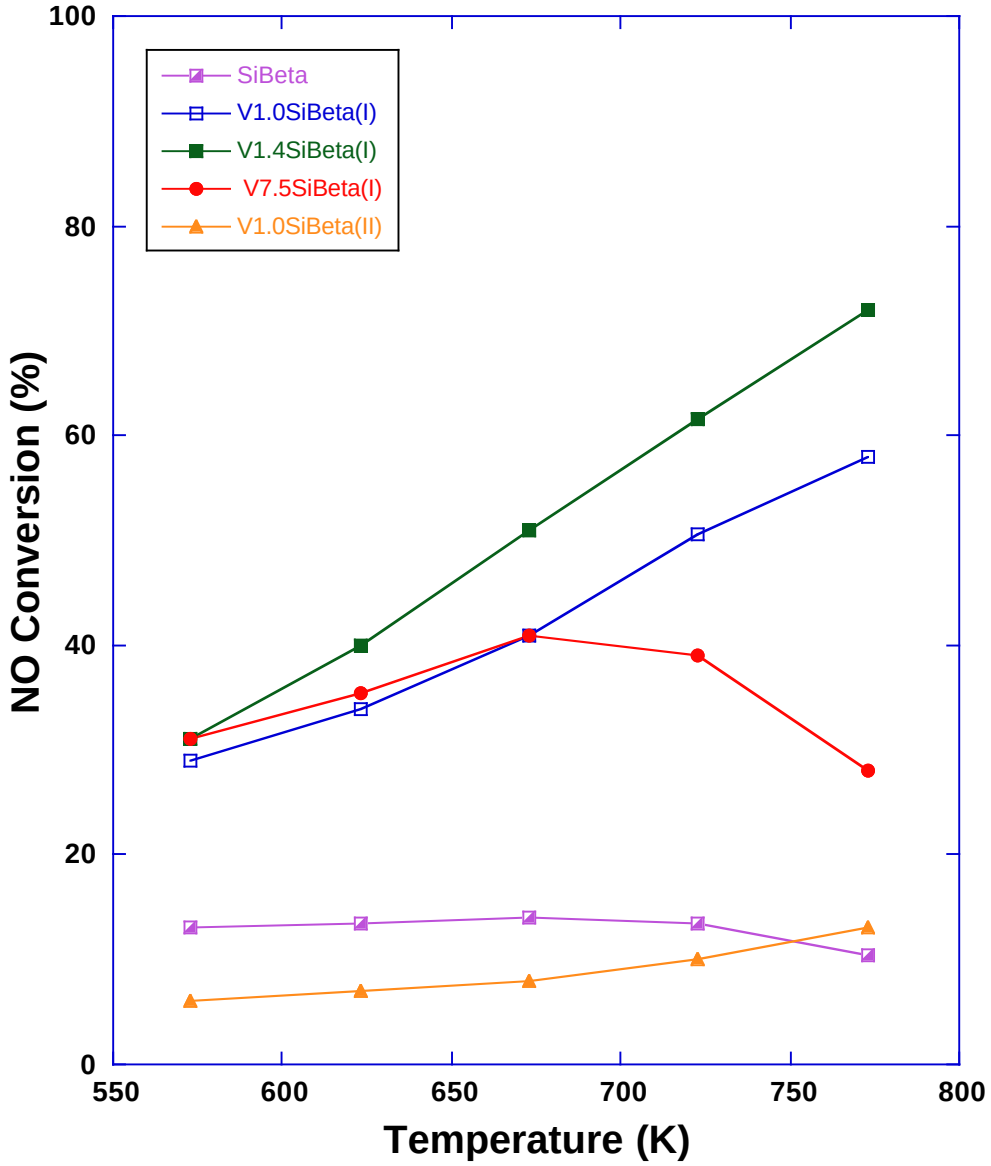

Figure 10. *Temperature-dependence of NO conversion in SCR of NO with ammonia on SiBeta, $V_{1.0}$SiBeta(I), $V_{1.4}$SiBeta(I), $V_{7.5}$SiBeta(I) and $V_{1.0}$SiBeta(II) zeolite catalysts. Composition of the feed: 1000 ppm NO, 1000 ppm NH_3, 3.5 vol.% O_2, 5.0 vol. % of water and He as balance.*

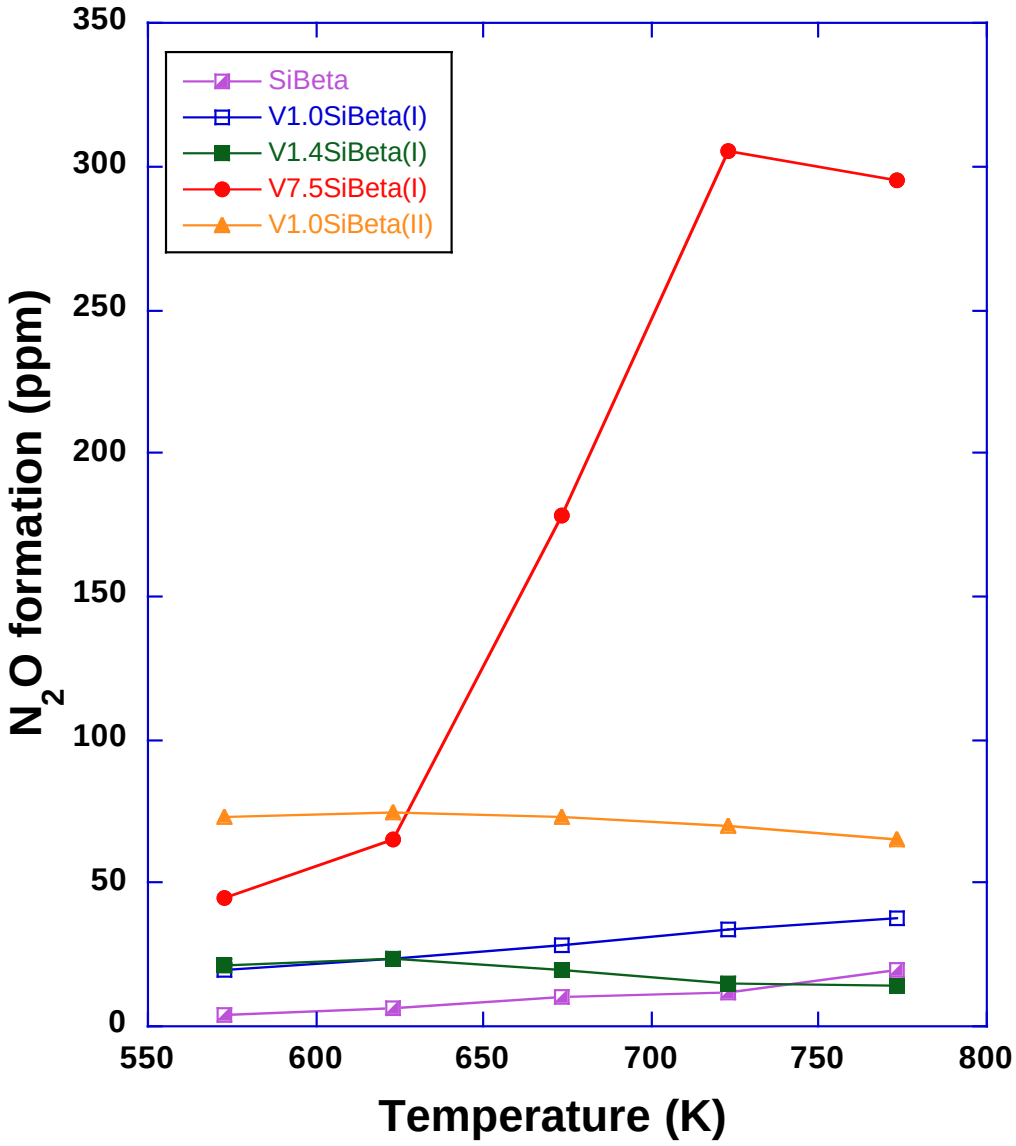

Figure 11. *Temperature-dependence of N_2O formation on SiBeta,$V_{1.0}$SiBeta(I), $V_{1.4}$SiBeta(I), $V_{7.5}$SiBeta(I) and $V_{1.0}$SiBeta(II) zeolite catalysts. Composition of the feed: 1000 ppm NO, 1000 ppm NH_3, 3.5 vol. % O_2, 5.0 vol. % of water and He as balance.*

As shown in Figure 10, SiBeta zeolite possesses very low activity in selective catalytic reduction of NO process with NO conversion lower than 14 % in the temperature range between 573 and 773 K. The incorporation of vanadium in SiBeta zeolite leads to a very important increase of the NO conversion into N_2 according to reaction (1):

$$4NH_3 + 4NO + O_2 = 4N_2 + 6H_2O \qquad (1)$$

As shown in Figure 10, the NO conversion depends on vanadium content, vanadium state and the reaction temperature. In the case of $V_{1.0}$SiBeta(I) and $V_{1.4}$SiBeta(I), containing mainly isolated pseudo-tetrahedral V(V) species conversion of NO increased with temperature and reached a maximum of almost 75 % at 773 K for $V_{1.4}$SiBeta(I).

For $V_{7.5}$SiBeta(I) catalyst, with the mixture of pseudo-tetrahedral and pseudo-octahedral V(V) species as evidenced by ^{51}V MAS NMR in Figure 4, the maximum NO conversion is obtained at 673 K (41 %) then strongly decreases down to 28 % at 773 K. This is probably related to a competitive reaction of ammonia oxidation to NO and N_2O according to the following (2) and (3) side reactions:

$$4NH_3 + 5O_2 = 4NO + 6H_2O \qquad (2)$$

$$2NH_3 + 2O_2 = N_2O + 3H_2O \qquad (3)$$

Reaction (3) leads to the N_2O formation that is an undesired product of SCR process. Such N_2O formation generally increases with increasing the reaction temperature and vanadium content, in particular with increasing amounts of pseudo-octahedral (V) species and polynuclear V species. For $V_{7.5}$SiBeta(I) catalyst containing pseudo-octahedral V(V) species, a huge increase in the formation of N_2O was observed, in particular at temperatures between 650 and 773 K (Figure 11). Considering that, simultaneously, a decrease of NO conversion occurs in this temperature range, it suggests that this by-product is probably generated by NH_3 oxidation (reaction (3)). We have separately checked the NH_3 oxidation of the catalysts studied in the absence of NO and we have observed much higher conversion of NH_3 in the presence of $V_{7.5}$SiBeta(I) than in the presence of $V_{1.0}$SiBeta(I) and $V_{1.4}$SiBeta(I) catalysts. Moreover, we have observed N_2O formation in this condition thus this confirm that N_2O is generated through oxidation route (reaction (3) in the manuscript).

On the other hand, the catalytic tests of $V_{1.0}$SiBeta(I) and $V_{1.4}$SiBeta(I) containing mainly pseudo-tetrahedral V(V) species lead to an extremely low formation of N_2O. It shows that the presence of pseudo-tetrahedral V(V) in V-containing SiBeta has a positive effect on SCR of NO with ammonia into N_2 (reaction 1).

In contrast, $V_{1.0}$SiBeta(II) and, especially, $V_{7.5}$SiBeta(I) catalyst containing pseudo-octahedral V(V) are much less active in SCR of NO process evidenced by low NO conversion (Figure 10) and high amount of N_2O is observed in the products, in particular for $V_{7.5}$SiBeta(I) at higher temperature range between 673 and 773 K (Figure 11), as a result of side oxidation of ammonia by gaseous oxygen (reactions 2-3). These results are in agreement with earlier reported works [50-51] showing that the pseudo-octahedral V(V) and, in particular, polynuclear V species, are much more active in oxidation of NH_3 by gaseous oxygen than in SCR of NO process into N_2. Moreover, our results suggest that, at high temperature range, the pseudo-octahedral V(V) species present in $V_{7.5}$SiBeta(I) are much less stable than pseudo-tetrahedral ones and thus both low NO conversion and selectivity to N_2 occur. The V-single site zeolites, $V_{1.0}$SiBeta(I) and $V_{1.4}$SiBeta(I) catalysts, containing isolated pseudo-tetrahedral V(V) species not only have very high selectivity to the desired product (N_2) but also give high NO conversion at 773 K.

Further studies are underway on VSiBeta(I) and VSiBeta(II) zeolites by *in situ* XAS, DR UV-Vis and EPR spectroscopies for a better description of the state of the vanadium species formed in both kinds of zeolite materials and of their catalytic activity in oxidative dehydrogenation of propane to propene.

Conclusions

The application of ^{51}V static and MAS NMR allowed determining the speciation of vanadium in initial aqueous NH_4VO_3 solutions as a function of pH and concentration, in the

supernatant after contacting siliceous Beta zeolite with aqueous NH_4VO_3 solutions and in wet solid prepared in these conditions.

The combined use of ^{51}V MAS NMR, ^{51}V 3Q MAS NMR, DR UV-vis, XPS and EPR allowed determining the state of vanadium in two series of V-containing SiBeta zeolite prepared at pH = 2.5 and 6 after different treatments.

As evidenced by ^{51}V MAS NMR, DR UV-vis and XPS in $V_{0.1}$SiBeta(I), $V_{0.5}$SiBeta(I), $V_{1.0}$SiBeta(I), $V_{1.4}$SiBeta(I), $V_{0.6}$SiBeta(II) and $V_{1.6}$SiBeta(II) vanadium was present mainly as pseudo-tetrahedral V(V) species.

In contrast, in $V_{1.0}$SiBeta(II) and $V_{7.5}$SiBeta(I), vanadium was present as pseudo-tetrahedral and pseudo-octahedral V(V) species.

As shown by XPS, the environment of V(V) in $V_{1.0}$SiBeta(I) sample remained almost unchanged after calcination in oxygen at 773 K and treatment in H_2 at 873 K suggesting that vanadium (V) species present in this sample were strongly bonded to zeolite structure.

In contrast, the environment of V(V) present in $V_{1.0}$SiBeta(II) changed upon calcination in oxygen at 773 K as well as upon treatment in H_2 at 873 K suggesting that vanadium species was less strongly bonded to zeolite structure.

Moreover, as shown by XPS and EPR spectroscopy, treatment of V_xSiBeta(I) and V_xSiBeta(II) with hydrogen at 873 K led to the change of oxidation state of vanadium from V to IV.

The catalytic activity of V-containing SiBeta zeolites in selective catalytic reduction of nitric oxide with ammonia as reducing agent strongly depended on the state of vanadium species created in Beta structure upon preparation.

The V-single site $V_{1.0}$SiBeta(I) and $V_{1.4}$SiBeta(I) catalysts with isolated pseudo-tetrahedral V(V) were active in SCR of NO process, with maximum NO conversion about 75 % at 773 K for $V_{1.4}$SiBeta(I) and with very low selectivity toward undesired N_2O.

In contrast, $V_{1.0}$SiBeta(II) and, especially, $V_{7.5}$SiBeta(I) catalysts containing pseudo-octahedral V(V) were much less active in SCR of NO process and high amount of undesired N_2O was produced at higher temperature range between 673 and 773 K, as a result of side oxidation of ammonia.

References

[1] S. Dzwigaj, E. Ivanova, R. Kefirov, K. Hadjiivanov, F. Averseng, J.M. Krafft, M. Che Catal. Today 142 (2009) 185-191. https://doi.org/10.1016/j.cattod.2008.09.031.

[2] A. Corma, Chem. Rev. 97 (1997) 2373-2419. https://doi.org/10.1021/cr960406n.

[3] G. Centi, F. Trifiro, Appl. Catal. A 143 (1996) 3-16. https://doi.org/10.1016/0926-860X(96)00067-1.

[4] S. Abonetti, F. Cavani, F. Trifiro, Catal. Rev. Sc. Eng. 38 (1996) 413-438. https://doi.org/10.1080/01614949608006463.

[5] T. Blasco, J.M. Lopez Nieto, Appl. Catal. A 157 (1997) 117-142. https://doi.org/10.1016/S0926-860X(97)00029-X.

[6] S. Dzwigaj, M. Che, B. Grzybowska, I. Gressel, K. Samson, Stud. Surf. Sci. Catal. 172 (2007) 385-388. eBook ISBN: 9780080932484.

[7] M. Trejda, M. Ziolek, Y. Millot, K. Chalupka, M. Che, S. Dzwigaj, J. Catal. 281 (2011) 169-176. https://doi.org/10.1016/j.jcat.2011.04.013.

[8] M. Iwamoto, H. Yahiro, K. Tanda, N. Mizuno, Y. Min, S. Kagawa, J. Phys. Chem., 95 (1991) 3727-3730. https://doi.org/10.1021/j100162a053.

[9] A. Penkova, K. Hadjiivanov, S. Dzwigaj, M. Che, J. Phys. Chem. C 111 (2007) 8623-8631. https://doi.org/10.1021/jp071927p.

[10] S. Dzwigaj, M. Che, Phys. Chem. B 110 (2006) 12490-12493. https://doi.org/10.1021/jp0623387.

[11] A. Mihaylova, K. Hadjiivanov, S. Dzwigaj, M. Che, J. Phys. Chem. B 110 (2006) 19530-19536. https://doi.org/10.1021/jp0634398.

[12] S. Dzwigaj, M.J. Peltre, P. Massiani, A. Davidson, M. Che, T. Sen, S. Sivasanker, J. Chem. Soc. Chem. Commun. (1998) 87-88. https://doi.org/10.1039/A704556E.

[13] S. Dzwigaj, M. Matsuoka, R. Franck, M. Anpo, M. Che, J. Phys. Chem. B 102 (1998) 6309-6312. https://doi.org/10.1021/jp981454+.

[14] S. Dzwigaj, M. Matsuoka, M. Anpo, M. Che, J. Phys. Chem. B 104 (2000) 6012-6020. https://doi.org/10.1021/jp0000331.

[15] F. Tielens, M. Trejda, M. Ziolek, S. Dzwigaj, Catal. Today 139 (2008) 221-226. https://doi.org/10.1016/j.cattod.2008.04.007.

[16] S. Dzwigaj, J. Janas, J. Mizera, J. Gurgul, R.P. Socha, M. Che, Catal. Lett 126 (2008) 36-42. https://doi.org/10.1007/s10562-008-9675-2.

[17] S. Dzwigaj, J. Janas, J. Gurgul, R.P. Socha, T. Shishido, M. Che, Appl. Catal. B 85 (2009) 131-138. https://doi.org/10.1016/j.apcatb.2008.07.003.

[18] J. Janas, W. Rojek, T. Shishido, S. Dzwigaj, Appl. Catal. B 123-124 (2012) 134-140. https://doi.org/10.1016/j.apcatb.2012.04.026.

[19] S. Dzwigaj, L. Stievano, F.E. Wagner, M. Che, J. Phys. Chem. Solids 68 (2007) 1885-1891. https://doi.org/10.1016/j.jpcs.2007.05.016.

[20] J. Janas, J. Gurgul, R.P. Socha, T. Shishido, M. Che, S. Dzwigaj, Appl. Catal. B 91 (2000) 113-122. https://doi.org/10.1016/j.apcatb.2009.05.013.

[21] R. Baran, J.M. Krafft, T. Onfroy, T. Grzybek, S. Dzwigaj, Micropor. Mesopor. Mater. 225 (2016) 515-523. https://doi.org/10.1016/j.micromeso.2015.12.061.

[22] J. Janas, T. Shishido, M. Che, S. Dzwigaj, Appl. Catal. B 89 (2009) 196-203. https://doi.org/10.1016/j.apcatb.2008.11.028.

[23] H.Y. Chen, W.M.H. Sachtler, Catal. Today 42 (1998) 73-83. https://doi.org/10.1016/S0920-5861(98)00078-9.

[24] G. Centi, F. Vazanna, Catal. Today 53 (1999) 683-693. https://doi.org/10.1016/S0920-5861(99)00155-8.

[25] Y. Li, J.N. Armor, Appl. Catal. B 2 (1993) 239-256. https://doi.org/10.1016/0926-3373(93)80051-E.

[26] M. Haneda, Y. Kintaichi, H. Shimada, H. Hamada, Journal of Catalysis 192 (2000) 137-148. https://doi.org/10.1006/jcat.2000.2831.

[27]] L.F. Cordoba, W.M.H. Sachtler, C.M. de Correa, Appl. Catal. B 56 (2005) 269–277. https://doi.org/10.1016/j.apcatb.2004.09.012.

[28] K. Arve, F. Klingstedt, K. Eranen, J. Warna, L.E. Lindfors, D.Yu. Murzin, Chem. Eng. J. 107 (2005) 215–220. https://doi.org/10.1016/j.cej.2004.12.031.

[29] T. Maunula, J. Ahola, H. Hamada, Appl. Catal. B 26 (2000) 173–192. https://doi.org/10.1016/S0926-3373(00)00118-1.

[30] T. Trejda, Y. Millot, K. Chalupka, S. Dzwigaj, Appl. Catal. A 579 (2019) 1-8. https://doi.org/10.1016/j.apcata.2019.04.009.

[31] A. Held, J. Kowalska-Kus, Y. Millot, F. Averseng, C. Calers, L. Valentin, S. Dzwigaj, J. Phys. Chem. C 122 (2018) 18570-18582. https://doi.org/10.1021/acs.jpcc.8b05731.

[32] J.P. Amoureux, L. Delevoye, S. Steuernagel, Z. Gan, S. Ganapathy, L. Montagne, J. Magn. Reson. 172 (2005) 268-278. https://doi.org/10.1016/j.jmr.2004.11.001.

[33] J.P. Amoureux, C. Fernandez, Solid State Nucl. Magn. Reson. 10 (1998) 211-223. https://doi.org/10.1016/S0926-2040(97) 00027-1.

[34] T. Spałek, P. Pietrzyk, Z. Sojka, J. Chem. Inf. Model. 45 (2005) 18–29. https://doi.org/10.1021/ci049863s.

[35] C.F. Base, Jr., R.E. Mesmer, Eds., The Hydrolysis of Cations, Wiley, New York, 1976, p. 210.

[36] A. Sigel, H. Sigel, Eds. Vanadium and Its Role for Life; Metal Ions In Biological Systems, Marcel Dekker, Inc.: New York. 1995, Vol. 31.

[37] A.K. Srivastava, J.L. Chiasson, Eds. Vanadium Compounds: Biochemical and Therapeutic Applications, Mol. Cell. Biochemistry, 1995, Vol. 153.

[38] D. Rehder, Vanadium in Biological Systems, N.D. Chasteen, Ed., Kluwer Academic Publishers: Dordrecht, The Nederlands, 1990, 173-197.

[39] R. Hajjar, Y. Millot, P.P. Man, M. Che, S. Dzwigaj, J. Phys. Chem. C 112 (2008) 20167-20175. https://doi.org/10.1021/jp808356q.

[40] S. Dzwigaj, P. Massiani, A. Davidson, M. Che, J. Mol. Catal. A 155 (2000) 169-182. https://doi.org/10.1016/S1381-1169(99)00332-5.

[41] S. Dzwigaj, M. Matsuoka, M. Anpo, M. Che, Catal. Lett. 72 **(**2001) 211-214. https://doi.org/10.1023/A:1009072908710.

[42] K. Hadjiivanov, G.N. Vayssilov, Adv. Catal. 47 (2002) 307-511. https://doi.org/10.1016/S0360-0564(02)47008-3.

[43] M. Hassan Zahedi-Niaki, S.M. Javaid Zaidi, S. Kaliaguine, Appl. Catal. A 196 (2000) 9-24. https://doi.org/10.1016/S0926-860X(99)00459-7.

[44] G. Grubert, J. Rathouský, G. Schulz-Ekloff, M. Wark, A. Zukal, Micropor. Mesopor. Mater. 22 (1998) 225-236. https://doi.org/10.1016/S1387-1811(98)00088-2.

[45] S. Youn, S. Jeong, D.H. Kim, Catal. Today 232 (2014) 185-191. https://doi.org/10.1016/j.cattod.2014.01.025.

[46] J.Y. Lee, S.H. Hong, S.P. Cho, S.C. Hong, Curr. Appl. Phys. 6 (2006) 996-1001. https://doi.org/10.1016/j.cap.2005.07.005.

[47] S. Dzwigaj, El.M. El Malki, M.J. Peltre, P. Massiani, A. Davidson, M. Che, Top. Catal. 11/12 (2000) 379-390. https://doi.org/10.1023/A:1027219107921.

[4] P. Pietrzyk, Z. Sojka, S. Dzwigaj, M. Che, J. Am. Chem. Soc. 129 (2007)

14174-14175. https://doi.org/10.1021/ja076689q.

[49] S. Dzwigaj, E. Ivanova, R. Kefirov, K. Hadjiivanov, F. Averseng, J.M. Krafft, M. Che, Catal. Today 142 (2009) 185-191. https://doi.org/10.1016/j.cattod.2008.09.031.

[50] L. Lietti, P. Forzatti, J. Catal. 147 (1994) 241-249. https://doi.org/10.1006/jcat.1994.1135.

[51] P. Forzatti, Appl. Catal. A 222 (2001) 221–236. https://doi.org/10.1016/S0926-860X(01)00832-8.